

Application of Real-time Time-dependent Density Functional Theory with the CVB3LYP Functional to Core Excitations

Tomoko Akama,¹ Yutaka Imamura,¹ and Hiromi Nakai^{*1,2}

¹Department of Chemistry and Biochemistry, School of Advanced Science and Engineering, Waseda University, Tokyo 169-8555

²Research Institute for Science and Engineering, Waseda University, Tokyo 169-8555

(Received January 18, 2010; CL-100049; E-mail: nakai@waseda.jp)

The CVB3LYP functional, which has been developed for evaluating both core and valence excitation energies with high accuracy, is applied to real-time time-dependent density functional theory (RT-TDDFT) calculations. The core excitation energies from the 1s orbitals of several second-row atoms obtained by RT-TDDFT with the CVB3LYP functional were demonstrated and compared with those of the frequency-domain TDDFT.

The time-dependent Hartree–Fock and time-dependent density functional theory (TDHF/TDDFT)^{1,2} are useful tools for excitation energy calculations in quantum chemistry because of their reasonable accuracy and computational cost. To obtain excitation energies and oscillator strengths, the most popular way is solving an eigenvalue problem in frequency-domain on the basis of excited configurations derived from the linear response of TDHF/TD Kohn–Sham (KS) equations.³ However, calculating high-lying excited states such as core excited states is time-consuming even though Davidson or Lanczos algorithms are adopted.

A real-time (RT) propagation of the TDHF/TDDFT equations is an alternative to calculate excited states. RT-TDHF/TDDFT calculations with real-space grids (for example, ref 4) and with plane waves (for example, ref 5) basis functions have been applied to valence excitations in the 1990s.^{4,5} The Gaussian basis functions have been also adopted during this decade.^{6–8} In a previous study,⁸ we showed that excitation energies obtained by RT-TDHF calculations are well accorded with frequency-domain TDHF results.

RT-TDDFT with the Gaussian basis functions can treat core excitations because they can describe localized orbitals. Exchange-correlation functionals capable of core excitations are very limited since the self-interaction severely underestimates⁹ core excitation energies with conventional functionals such as B3LYP.¹⁰ The assessments revealed that BHHLYP functional,¹¹ which uses 50% HF exchange, can accurately describe core excitations and that B3LYP, which uses 20% HF exchange, can describe valence excitations. Based on the assessments, two different kinds of functionals for core excitations have been proposed: pure¹² and hybrid functionals.^{13,14}

The hybrid functional core–valence B3LYP (CVB3LYP) uses appropriate ratios of HF exchange for core and valence excitations. Specifically, the CVB3LYP total energy is decomposed into core–core (CC), core–valence (CV), and valence–valence (VV) interactions. The coefficients of CC and VV were set to those of BHHLYP and B3LYP, respectively. The coefficients of CV interactions were set to the average values of those of BHHLYP and B3LYP. The Fock operators for the CVB3LYP are represented as:

$$F_C = h + 2J - (a_{CC}K_C + a_{CV}K_{OV}) + (b_{CC} - b_{CV})V_{xc}[\rho_C] + b_{CV}V_{xc}[\rho] \quad (1)$$

$$F_{OV} = h + 2J - (a_{CV}K_C + a_{VV}K_{OV}) + (b_{VV} - b_{CV})V_{xc}[\rho_{OV}] + b_{CV}V_{xc}[\rho] \quad (2)$$

h , J , and K , are one-electron, Coulomb, and HF exchange operators, respectively. V represents the exchange-correlation potential. a and b are the coefficients of HF exchange and exchange-correlation functional, respectively. ρ , ρ_C , and ρ_{OV} are the densities of all occupied, core, and occupied valence orbitals, respectively. To guarantee invariance under unitary transformation between core and occupied valence orbitals, Roothaan's coupling operator¹⁵ was used, which is often adopted in restricted open-shell HF calculations. Further details of CVB3LYP and TDDFT procedures with CVB3LYP are given in ref 13. The CVB3LYP functional is useful for accurately reproducing not only core but also valence excitation energies and applied to core excitations of nucleobases.¹⁶

In this paper, we applied the CVB3LYP functional to the RT-TDKS calculations with Gaussian basis functions. The TDKS equation is written as the equation of motion in terms of the time-dependent density matrix, $\mathbf{D}(t)$, and its first-order term is represented as follows:

$$i \frac{\partial}{\partial t} \delta \mathbf{D}^{(1)}(t) = [\mathbf{F}^{(0)}, \delta \mathbf{D}^{(1)}(t)] + [\delta \mathbf{F}^{(1)}(t), \mathbf{D}^{(0)}] + [\mathbf{V}^{\text{ext}}(t), \mathbf{D}^{(0)}] \quad (3)$$

where the orthonormal spatial bases $\{\phi_i(\mathbf{r})\}$ are adopted. Here, $\mathbf{D}^{(0)}$ and $\delta \mathbf{D}^{(1)}(t)$ are the static and first-order induced density matrices, while $\mathbf{F}^{(0)}$ and $\delta \mathbf{F}^{(1)}(t)$ are those of Fock matrices, respectively. An element of the interaction matrix between the electron and external field, $\mathbf{V}^{\text{ext}}(t)$, is

$$V_{ij}^{\text{ext}}(t) = \varepsilon(t) \mathbf{e}^{\text{ext}} \cdot \langle \phi_i | \mathbf{r} | \phi_j \rangle \quad (4)$$

where $\varepsilon(t)$ and \mathbf{e}^{ext} are the time-dependent part and unit vector of the external field, and $\langle \phi_i | \mathbf{r} | \phi_j \rangle$ is the dipole integral. Equation 3 corresponds to the linear response, which is usually adopted in the frequency domain calculation. We obtain an excitation spectrum as the imaginary part of the Fourier transformation (FT) of the induced polarizations, $\delta \mathbf{P}(t)$, which is constructed from $\delta \mathbf{D}(t)$ under the dipole approximation.

Numerical applications to small molecules were performed and compared to frequency-domain TDDFT and experimental results. The RT-TDDFT calculations were performed using a modified version of the GAMESS program¹⁷ linked to a original RT-TDHF/TDDFT code, which has been implemented in the previous study.⁸ The external field was set to $\varepsilon(t) = \delta(t)$ and $\mathbf{e}^{\text{ext}} = (1, 1, 1)$. As it was demonstrated that the effect of the

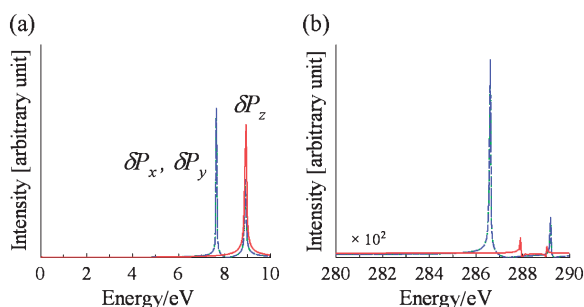


Figure 1. Excitation spectra of acetylene obtained by applying an FT analysis to the induced polarization vector of the RT-TD-CVB3LYP/6-31+G** calculations. (b) Core excitation spectrum is scaled up 10^2 times from (a) valence one.

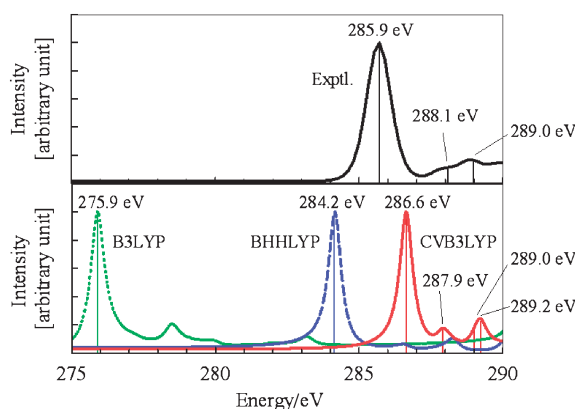


Figure 2. Core excitation spectra of acetylene obtained by the experiment²⁰ and RT-TDDFT/6-31+G** calculations.

Table 1. Valence and core excitation energies E_{excit} of acetylene obtained by RT-TDDFT/6-31+G** calculations with CVB3LYP functional (RT-TD-CVB3LYP) and FT analysis^a

	Polarization direction	RT-TD-CVB3LYP		Frequency-domain TD-CVB3LYP		
		$E_{\text{excit}}/\text{eV}$	(diff.)	$E_{\text{excit}}/\text{eV}$	Oscillator strength	Main configuration
Valence	x, y	7.65 ^a	(-0.01)	7.66	0.099	$\pi \rightarrow 3s\sigma_g$
	x, y		(-0.04)	7.69	$<1.5 \times 10^{-6}$	$\pi \rightarrow 3s\sigma_u$
	x, y	8.89	(-0.02)	8.91	0.149	$\pi \rightarrow \sigma^*$
	z	8.89	(-0.03)	8.92	0.668	$\pi \rightarrow \pi^*$
Core	x, y	286.60	(0.01)	286.59	0.074	C $1s\sigma_u \rightarrow \pi^*$
	z	287.89 ^b	(0.03)	287.87	0.010	C $1s\sigma_u \rightarrow 3s\sigma_g$
	z		(0.02)	287.87	$<1.5 \times 10^{-6}$	C $1s\sigma_u \rightarrow 3s\sigma_u$
	z	288.10 ^b	(-0.00)	288.10	0.001	C $1s\sigma_g \rightarrow 3s\sigma_u$
	z		(-0.00)	288.10	$<1.65 \times 10^{-5}$	C $1s\sigma_g \rightarrow 3s\sigma_g$
	z	289.03	(0.02)	289.01	0.014	C $1s\sigma_u \rightarrow \sigma^*$
	x, y	289.19	(0.01)	289.18	0.013	C $1s\sigma_g \rightarrow 3p\pi_g$

^aThe differences from the frequency-domain results are shown in parentheses. ^bCorresponding to two quasidegenerate excitations.

core-correlation basis set is small in the TDDFT calculations with the CVB3LYP functional,¹³ the 6-31G** basis set¹⁸ was adopted in this study except for the acetylene calculation where the 6-31+G** basis set^{18,19} was adopted.

Figure 1 shows the excitation spectra for (a) valence (0–10 eV) and (b) core (280–290 eV) excitations of acetylene (parallel to z axis) obtained by RT-TD-CVB3LYP. Simulations were carried out over $t = -0.1$ to 80 femtosecond (fs) with the time step of $\Delta t = 5 \times 10^{-4}$ fs. The horizontal axis represents the energy, $\hbar\omega$ (in eV), with a resolution of 0.052 eV, and the vertical axis represents the intensity as an absolute value, $|\text{Im}[\delta P_{\xi}(\omega)]|$ ($\xi = x, y, z$) (in arbitrary units). Because of the symmetry of the acetylene molecule, δP_x and δP_y are equivalent. The peak positions correspond to the excitation energies, and their numerical data are summarized in Table 1. The dipole-allowed excitation energies, oscillator strengths, and main configurations from conventional frequency-domain TD-CVB3LYP calculations are tabulated. The excitation energy differences between RT and conventional results are also shown in parentheses. The excitation energies for the dipole-allowed transitions obtained by the RT-TD-CVB3LYP calculations agree with the conventional TD-CVB3LYP results within errors of 0.04 and 0.03 eV for valence and core excitations, respectively, which are less than the resolution. It should be noted that the peak at 7.65 eV corresponds to two excitations from π to $3s\sigma_g$ and $3s\sigma_u$ (Rydberg) orbitals because these excitations have the energy difference of 0.03 eV, which is less than the resolution. In

a similar way, the peaks at 287.89 and 288.10 eV include two excitations to $3s\sigma_g$ and $3s\sigma_u$ orbitals with the energy difference less than 0.01 eV. These excitations can be separated from each other when the longer simulation is performed to obtain the spectrum with higher resolution.

Next, the RT-TDDFT results with B3LYP, BHHLYP, and CVB3LYP functionals are compared with the experimental results. Figure 2 shows the core excitation spectra (275–290 eV) of acetylene obtained experimentally²⁰ and theoretically. The theoretical spectra were obtained by multiplying RT-TDDFT results $|\text{Im}[\delta P(\omega)]|$ by the Lorentzian function with the half width of 0.25 eV and normalized on the intensity of the main peaks corresponding to the C $1s\sigma_u \rightarrow \pi^*$ excitations at 275.90, 284.16, and 286.60 eV for B3LYP, BHHLYP, and CVB3LYP functionals, respectively. The spectrum by the B3LYP functional is significantly different from the experimental one. The peak position of the C $1s\sigma_u \rightarrow \pi^*$ excitation is underestimated with the deviation of 10.0 eV. The spectrum by the BHHLYP functional reproduces the excitation energy with the deviation of 1.7 eV, while the CVB3LYP functional further reduces the deviation to 0.7 eV. The second and third peaks in the experimental spectrum were assigned to the core excitations to $3s$ and $3p$ orbitals, respectively.²⁰ The CVB3LYP functional provides the corresponding peaks with the deviations of 0.2 eV, as shown in Table 1. As a result, the shape of the spectrum by the CVB3LYP functional becomes closer to the experimental one than the other functionals.

Table 2. $1s \rightarrow \pi^*$ excitation energies (in eV) of CH_2O , CO , CF_2O , N_2 , and N_2O molecules obtained by RT-TDDFT/6-31G** calculations with BHHLYP and CVB3LYP functionals^a

Molecule	Main configuration	RT-TD-BHHLYP	RT-TD-CVB3LYP	Exptl.
CH_2O	C $1s \rightarrow \pi^*$	283.50 (-2.53)	286.60 (0.57)	286.03 ^b
CO	C $1s \rightarrow \pi^*$	283.91 (-3.49)	287.43 (0.03)	287.4 ^b
CF_2O	C $1s \rightarrow \pi^*$	288.15 (-2.74)	291.56 (0.67)	290.89 ^b
N_2	N $1s \rightarrow \pi^*$	398.58 (-2.38)	401.99 (1.03)	400.96 ^c
N^+NO	N $1s \rightarrow \pi^*$	399.20 (-1.90)	402.30 (1.20)	401.1 ^d
NN^+O	N $1s \rightarrow \pi^*$	402.40 (-2.30)	405.71 (1.01)	404.7 ^d
CH_2O	O $1s \rightarrow \pi^*$	528.75 (-2.05)	532.26 (1.46)	530.8 ^b
CF_2O	O $1s \rightarrow \pi^*$	530.81 (-1.89)	533.91 (1.21)	532.7 ^b
CO	O $1s \rightarrow \pi^*$	532.36 (-1.84)	535.36 (1.16)	534.2 ^b
N_2O	O $1s \rightarrow \pi^*$	533.71 (-0.89)	535.88 (1.28)	534.6 ^b
CF_2O	F $1s \rightarrow \pi^*$	686.90 (-2.30)	688.28 (-0.92)	689.2 ^b

^aThe deviations from the experimental results are shown in parentheses. ^bref 21. ^cref 22. ^dref 23.

Finally, the energies of core excitations from several second-row atoms obtained by the RT-TD-CVB3LYP and RT-TD-BHHLYP calculations are compared to the experimental data.^{21–23} Table 2 shows the dipole-allowed $X1s \rightarrow \pi^*$ excitation energies ($X = \text{C}, \text{N}, \text{O}$, and F) of formaldehyde (CH_2O), carbon monoxide (CO), carbonic difluoride (CF_2O), nitrogen (N_2), and nitrous oxide (N_2O) molecules obtained by RT-TDDFT calculations with the BHHLYP and CVB3LYP functionals. Simulations were carried out over $t = -0.1$ to 40 fs with the time step of $\Delta t = 2 \times 10^{-4}$ fs. C, N, O, and F in bold face correspond to atoms whose $1s$ electrons are excited. The deviations from the experimental values are shown in parentheses. The core excitation energies of RT-TD-BHHLYP calculations are underestimated with the deviations of 1.8–3.5 eV. On the other hand, those of RT-TD-CVB3LYP calculations showed better performance with the deviations less than 1.5 eV. Although the deviations are rather larger than those of the previous study,²¹ the use of higher basis sets can significantly reduce the deviations to about 0.3 eV as shown in ref 13. Moreover, the incorporation of electron correlation may realize the performance comparable to that of the previous study.²¹

In conclusion, application of the CVB3LYP functional to the RT-TDDFT calculations enabled evaluation of core and valence excitations with high accuracy. In the previous study,⁸ we have clarified that the picture of the electron dynamics is provided by the short-time Fourier transform (STFT) analysis of RT-TDHF/TDDFT results. Its extension to the RT-TD-CVB3LYP calculation is promising for understanding core excitation electron dynamics.

Some of the present calculations were performed at the Research Center for Computational Science (RCCS), Okazaki Research Facilities, National Institutes of Natural Sciences (NINS). This study was partially supported by a Grant-in-Aid for Scientific Research on Priority Areas “Molecular Theory for Real Systems” KAKENHI 18066016 from the Ministry of Education, Culture, Sports, Science and Technology (MEXT), Japan; by the Nanoscience Program in the Next Generation Super Computing Project of the MEXT; by the Global Center Of Excellence (GCOE) “Practical Chemical Wisdom” from the MEXT; by a Waseda University Grant for Special Research Projects (Project number: 2009B-102); and by a project research grant for the “Development of High-performance Computational Environment for Quantum Chemical Calculation and its Assessment” from the Research Institute for Science and Engineering

(RISE), Waseda University. One of the authors (TA) is indebted to a Research Fellowship for Young Scientists from the Japan Society for the Promotion of Science (JSPS).

References

- P. A. M. Dirac, *Proc. Cambridge Philos. Soc.* **1930**, *26*, 376.
- E. Runge, E. K. U. Gross, *Phys. Rev. Lett.* **1984**, *52*, 997; E. K. U. Gross, W. Kohn, *Adv. Quantum Chem.* **1990**, *21*, 255; M. A. L. Marques, E. K. U. Gross, in *A Primer in Density Functional Theory*, ed. by C. Fiolhais, F. Nogueira, M. A. L. Marques, Springer, New York, **2003**, p. 144.
- M. E. Casida, in *Recent Advances in Density Functional Methods*, ed. by D. P. Chong, World Scientific, Singapore, **1995**, Vol. 1, p. 155; R. E. Stratmann, G. E. Scuseria, M. J. Frisch, *J. Chem. Phys.* **1998**, *109*, 8218.
- K. Yabana, G. Bertsch, *Phys. Rev. B* **1996**, *54*, 4484.
- O. Sugino, Y. Miyamoto, *Phys. Rev. B* **1999**, *59*, 2579.
- C. Y. Yam, S. Yokojima, G. H. Chen, *J. Chem. Phys.* **2003**, *119*, 8794; C. Y. Yam, S. Yokojima, G. H. Chen, *Phys. Rev. B* **2003**, *68*, 153105; F. Wang, C. Y. Yam, G. H. Chen, K. Fan, *J. Chem. Phys.* **2007**, *126*, 134104.
- J. Sun, J. Song, Y. Zhao, W.-Z. Liang, *J. Chem. Phys.* **2007**, *127*, 234107; Z. Guo, W. Z. Liang, Y. Zhao, G. H. Chen, *J. Phys. Chem. C* **2008**, *112*, 16655.
- T. Akama, H. Nakai, *J. Chem. Phys.* **2010**, *132*, 054104.
- Y. Imamura, T. Otsuka, H. Nakai, *J. Comput. Chem.* **2007**, *28*, 2067; Y. Imamura, H. Nakai, *Int. J. Quantum Chem.* **2007**, *107*, 23.
- A. D. Becke, *J. Chem. Phys.* **1993**, *98*, 5648.
- A. D. Becke, *J. Chem. Phys.* **1993**, *98*, 1372.
- Y. Imamura, H. Nakai, *Chem. Phys. Lett.* **2006**, *419*, 297.
- A. Nakata, Y. Imamura, T. Otsuka, H. Nakai, *J. Chem. Phys.* **2006**, *124*, 094105.
- A. Nakata, Y. Imamura, H. Nakai, *J. Chem. Phys.* **2006**, *125*, 064109; A. Nakata, Y. Imamura, H. Nakai, *J. Chem. Theory Comput.* **2007**, *3*, 1295.
- C. C. J. Roothaan, *Rev. Mod. Phys.* **1960**, *32*, 179; S. Huzinaga, *Bunshikidouhou*, Iwanami Shoten, Tokyo, **1980**; K. Hirao, H. Nakatsuji, *J. Chem. Phys.* **1973**, *59*, 1457.
- T. Tsuchimochi, M. Kobayashi, A. Nakata, Y. Imamura, H. Nakai, *J. Comput. Chem.* **2008**, *29*, 2311; A. Thompson, S. Saha, F. Wang, T. Tsuchimochi, A. Nakata, Y. Imamura, H. Nakai, *Bull. Chem. Soc. Jpn.* **2009**, *82*, 187.
- M. W. Schmidt, K. K. Baldrige, J. A. Boatz, S. T. Elbert, M. S. Gordon, J. H. Jensen, S. Koseki, N. Matsunaga, K. A. Nguyen, S. Su, T. L. Windus, M. Dupuis, J. A. Montgomery, *J. Comput. Chem.* **1993**, *14*, 1347.
- W. J. Hehre, R. Ditchfield, J. A. Pople, *J. Chem. Phys.* **1972**, *56*, 2257; P. C. Hariharan, J. A. Pople, *Theor. Chim. Acta* **1973**, *28*, 213.
- T. Clark, J. Chandrasekhar, G. W. Spitznagel, P. v. R. Schleyer, *J. Comput. Chem.* **1983**, *4*, 294.
- A. P. Hitchcock, C. E. Brion, *J. Electron Spectrosc. Relat. Phenom.* **1977**, *10*, 317; Gas Phase Core Excitation Database on the McMaster University Web site <http://unicorn.mcmaster.ca/corex/cedb-title.html>.
- C.-H. Hu, D. P. Chong, *Chem. Phys. Lett.* **1996**, *262*, 729.
- M. Ohno, P. Decleva, G. Fronzoni, *Surf. Sci.* **1993**, *284*, 372.
- G. R. Wight, C. E. Brion, *J. Electron Spectrosc. Relat. Phenom.* **1974**, *3*, 191.